Mixing using multi-body decays at LHCb

Stefanie Reichert[*] **on behalf of the LHCb collaboration**
Technische Universität Dortmund
E-mail: stefanie.reichert@cern.ch

Multi-body D^0 decays provide important insights into the phenomenon of charm mixing as some of those observables are complementary to those from two-body decay modes. In these multi-body channels, the interference between different resonant contributions can be exploited using either model-dependent or model-independent methods to determine the mixing parameters x and y. In this contribution, the latest results on charm mixing from multi-body decays from LHCb are presented.

VIII International Workshop On Charm Physics
5-9 September, 2016
Bologna, Italy

---

[*]Speaker.

1. Introduction

Neutral meson mixing has been observed in the K^0, B^0, B_s^0 and the D^0 systems and is caused by non-vanishing differences in mass $\Delta m \equiv m_2 - m_1$ or width $\Delta\Gamma \equiv \Gamma_2 - \Gamma_1$ of the physical eigenstates $|M_{1,2}\rangle$, which do not coincide with the flavour eigenstates $|M^0\rangle$ and $|\bar{M}^0\rangle$. In contrast to mixing in the kaon and beauty sector, charm mixing is expected to be small. The short distance $|\Delta F| = 2$ contributions to mixing between D^0 and $\bar{D}^0$ mesons are CKM-suppressed ($\propto \lambda^5$) and due to the small mass difference between s and d quarks further suppressed by the GIM mechanism [1]. In addition, contributions from long range hadronic interactions impact the charm mixing parameters. The current world averages of the charm mixing parameters are $x = (0.37 \pm 0.16) \times 10^{-2}$ and $y = (0.66^{+0.07}_{-0.10}) \times 10^{-2}$ as extracted from a global fit allowing for *CP* violation [2]. Whereas the mixing parameter y differs by 7.8σ from zero, the situation on x is less evident as the deviation from zero is about 2.3σ.

In this contribution, the first model-independent measurement of the charm mixing parameters in $D^0 \to K_S^0 \pi^+ \pi^-$ decays on a dataset corresponding to an integrated luminosity of $1\,\text{fb}^{-1}$ recorded with the LHCb detector [3] at a centre-of-mass energy of $\sqrt{s} = 7\,\text{TeV}$ is presented. Furthermore, a measurement of charm mixing in the four-body final state $D^0 \to K^+ \pi^- \pi^+ \pi^-$ is presented, providing input parameters for a measurement of the CKM angle γ in $B^\pm \to DK^\pm$ with $D \to K^\mp \pi^\pm \pi^\mp \pi^\pm$ decays. The latter measurement relies on a dataset of $3\,\text{fb}^{-1}$ taken at centre-of-mass energies of 7 and 8 TeV in 2011 and 2012, respectively.

2. Model-independent mixing measurement in $D^0 \to K_S^0 \pi^+ \pi^-$

The decay channel $D^0 \to K_S^0 \pi^+ \pi^-$ allows to study both Cabibbo-favoured (CF) and doubly Cabibbo-suppressed (DCS) components and hence, the strong phase difference $\Delta\delta_D$ between the amplitudes contributing to the $K_S^0 \pi^+ \pi^-$ final state is measurable. The analysis of $D^0 \to K_S^0 \pi^+ \pi^-$ decays allows to disentangle the effects of the strong phase difference and the mixing parameters x and y, which enables a model-independent measurement [5] of the mixing parameters by using average $\Delta\delta_D$ measurements provided by the CLEO collaboration [4]. These measurements are performed in 16 two-dimensional bins in the Dalitz plane spanned by $m^2(K_S^0 \pi^+) \equiv m_{12}^2$ and $m^2(K_S^0 \pi^-) \equiv m_{13}^2$, which are symmetric with respect to the $m^2(\pi^+ \pi^-)$ axis as illustrated in Fig. 1. The phase-space dependent amplitudes $\mathscr{A}_{D^0}$ and $\mathscr{A}_{\bar{D}^0}$ corresponding to the decay of a D^0 or $\bar{D}^0$ candidate to a point (m_{12}^2, m_{13}^2) are

$$\mathscr{A}_{\bar{D}^0}(m_{12}^2, m_{13}^2) = \mathscr{A}_{D^0}(m_{13}^2, m_{12}^2), \tag{2.1}$$

assuming no direct *CP* violation. The time-dependence of the amplitude of an initial D^0 (similar for $\bar{D}^0$ decays) is hence

$$\begin{aligned}
\mathscr{A}_{D^0}(m_{12}^2, m_{13}^2, t) &= \mathscr{A}_{D^0}(m_{12}^2, m_{13}^2) g_+(t) \\
&+ \frac{q}{p} \mathscr{A}_{\bar{D}^0}(m_{13}^2, m_{12}^2) g_-(t), \quad \text{with}
\end{aligned} \tag{2.2}$$

$$g_\pm(t) = \frac{1}{2} \left(e^{-i(m_2 - i\Gamma_2/2)t} \pm e^{-i(m_1 - i\Gamma_1/2)t} \right). \tag{2.3}$$

The corresponding probability density $\mathscr{P}_{D^0}$ is given by the normalised modulus squared of the time-dependent amplitude $\mathscr{A}_{D^0}(m_{12}^2, m_{13}^2, t)$, which is expanded at leading order in x and y assuming $q/p = 1$ to

$$\mathscr{P}_{D^0}(m_{12}^2, m_{13}^2, t) = \Gamma e^{-\Gamma t} \left[|\mathscr{A}_{D^0}|^2 - \Gamma t \mathrm{Re}\left(\mathscr{A}_{D^0}^* \mathscr{A}_{\bar{D}^0}(y + ix)\right) \right]. \tag{2.4}$$

The phase-space integral of the probability density in bin i in the Dalitz plane as defined in Fig. 1 equals

$$\mathscr{P}_{D^0}(i; t) = \int_i \mathscr{P}_{D^0}(m_{12}^2), m_{13}^2, t) dm_{12}^2 dm_{13}^2 \tag{2.5}$$

$$= \Gamma e^{-\Gamma t} \left\{ T_i - \Gamma t \sqrt{T_i T_{-i}} (y c_i + x s_i) \right\}, \tag{2.6}$$

where the following definitions apply

$$T_i = \int_i |\mathscr{A}_{D^0}|^2 dm_{12}^2 dm_{13}^2, \tag{2.7}$$

$$c_i = \frac{1}{\sqrt{T_i T_{-i}}} \int_i |\mathscr{A}_{D^0}^*| |\mathscr{A}_{\bar{D}^0}| \cos(\Delta\delta_D) dm_{12}^2 dm_{13}^2, \tag{2.8}$$

$$s_i = -\frac{1}{\sqrt{T_i T_{-i}}} \int_i |\mathscr{A}_{D^0}^*| |\mathscr{A}_{\bar{D}^0}| \sin(\Delta\delta_D) dm_{12}^2 dm_{13}^2. \tag{2.9}$$
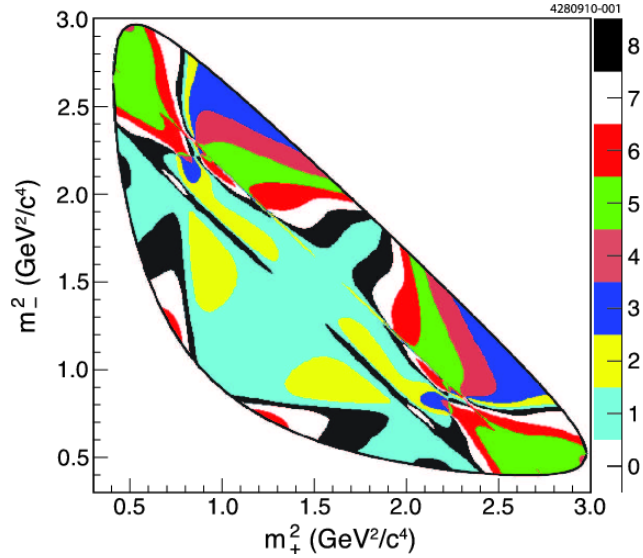

Figure 1: Binned measurements of the strong phase difference $\Delta\delta_D$ from CLEO for the equal $\Delta\delta_D$ BaBar 2008 model [4]. The phase space binning in $m_+^2 \equiv m^2(K_S^0 \pi^+)$ and $m_-^2 \equiv m^2(K_S^0 \pi^-)$ is chosen to minimise the variation of $\Delta\delta_D$ in each bin.

The parameters T_i, c_i, s_i are provided by CLEO [4] allowing for a model-independent determination of the mixing parameters x and y. This measurement is performed on a dataset recorded at a centre-of-mass energy of $\sqrt{s} = 7\,\text{TeV}$, which corresponds to an integrated luminosity of $1\,\text{fb}^{-1}$. The $D^0 \to K_S^0 \pi^+ \pi^-$ decays are required to originate from a $D^{*+} \to D^0 \pi^+$ decay produced promptly in the pp collision. After a trigger and cut-based selection, the yield of signal candidates is determined from an extended maximum likelihood fit to the distribution of the D^0 mass, m_D, shown in Fig. 2. The total signal yield is found to be 178k candidates with a purity of $(97.4 \pm 0.3)\%$.
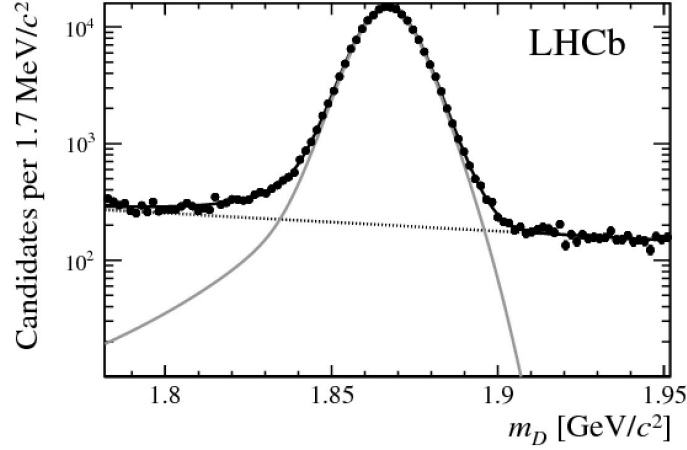

Figure 2: Fitted m_D distribution to extract the signal and combinatorial background contributions. Displayed is the data (black dots), the total fit model (solid black line), the combinatorial background component (dotted line), and the signal component (grey) [5].

The mixing parameters are extracted from a multi-stage fit procedure. In the first afore mentioned stage, the shapes of the signal and combinatorial background distributions are determined. As a main background component arises from secondary decays of B mesons, the background shape of these decays is determined from a two-dimensional maximum likelihood fit of the D^0 decay time, t_D, and $\ln(\chi^2_{\text{IP}})$ using the mass sidebands to estimate background contributions. The observable $\ln(\chi^2_{\text{IP}})$, which is the difference in the vertex fit χ^2 of the primary pp vertex reconstructed with and without the D^0 candidate, allows to distinguish between prompt and secondary decays. An exemplary projection of the fit result on $\ln(\chi^2_{\text{IP}})$ is illustrated in Fig. 3. After determining the shapes of the combinatorial and secondary background components, extended maximum likelihood fits are performed to m_D and $\delta m \equiv m_{D^*} - m_D$ in each phase-space bin separately for datasets of D^{*+} and D^{*-} candidates to obtain the signal and background yields. The mixing parameters are then extracted from simultaneous maximum likelihood fits based on $\mathscr{P}_{D^0}$ (and $\mathscr{P}_{\bar{D}^0}$) to $(t_D, \ln(\chi^2_{\text{IP}}))$ exploiting the information obtained from the previous fits. The mixing parameters are found to be

$$x = (-0.86 \pm 0.53 \pm 0.17) \times 10^{-2}, \qquad (2.10)$$

$$y = (0.03 \pm 0.46 \pm 0.13) \times 10^{-2}, \qquad (2.11)$$

3

where the uncertainties are statistical and systematic, respectively. The dominant systematic uncertainties arise from the CLEO inputs, especially from T_i, resolution effects and from backgrounds.
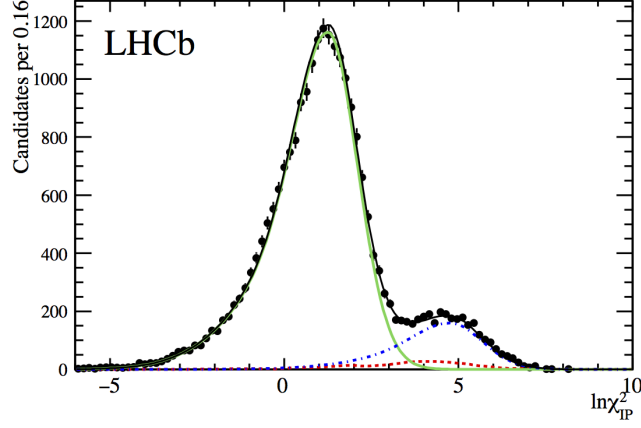

Figure 3: Exemplary $\ln(\chi^2_{\text{IP}})$ distribution used to separate prompt signal from secondary background candidates for $1.05 < t_D < 1.35\,\text{ps}$. A fit to data (black dots) has been performed with a model (solid black line) consisting of a prompt component (solid green line), background from secondaries (dot-dashed blue line) and a combinatorial background component (dashed red line) [5].

3. Mixing in $D^0 \to K^+\pi^-\pi^+\pi^-$

Charm mixing has also been studied in a four-body final state by measuring the time-dependent ratio $R(t)$ of wrong-sign $D^0 \to K^+\pi^-\pi^+\pi^-$ to right-sign $D^0 \to K^-\pi^+\pi^-\pi^+$ decays [6], which is

$$R(t) \approx (r_D^{K3\pi})^2 - r_D^{K3\pi} R_D^{K3\pi} y'_{K3\pi} \Gamma t + \frac{x^2 + y^2}{4}(\Gamma t)^2, \tag{3.1}$$

neglecting higher order terms in t/τ and assuming that *CP* symmetry holds. Here, $r_D^{K3\pi}$ refers to the phase-space averaged ratio of DCS to CF amplitudes, $R_D^{K3\pi}$ denotes the coherence factor, and $y'_{K3\pi} \equiv y\cos(\Delta\delta_D^{K3\pi}) - x\sin(\Delta\delta_D^{K3\pi})$ with $\Delta\delta_D^{K3\pi}$ being the strong phase difference. The results of this measurement provide crucial input for a measurement of the CKM angle γ in the channel $B^\pm \to D(\to K^\mp\pi^\pm\pi^\mp\pi^\pm)K^\pm$. The analysed datasets were recorded in 2011 and 2012 at centre-of-mass energies of 7 and 8 TeV, respectively, corresponding to an overall integrated luminosity of $3\,\text{fb}^{-1}$. The selected D^0 candidates originate from a prompt $D^{*+} \to D^0\pi^+$ decay allowing to exploit the mass difference between the D^* and D^0 candidates, Δm, to extract the signal yields for both right-sign and wrong-sign datasets. Figure 4 shows the Δm distributions with the binned likelihood fits superimposed, which yields 11.4 million right-sign and 43k wrong-sign candidates after applying a trigger and selection.
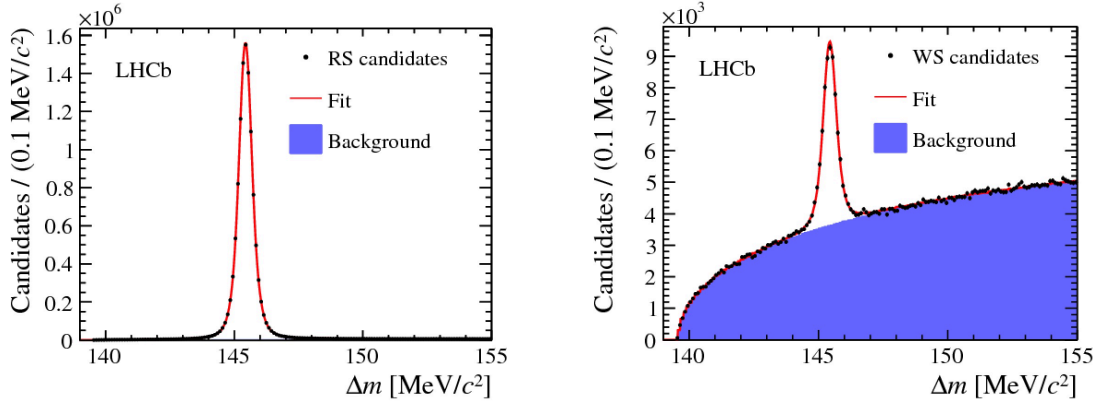
Figure 4: Fitted Δm distributions to right-sign (left) and wrong-sign (right) candidates. The fit model contains a signal and a combinatorial background component [6].

The time-dependent ratio of wrong-sign to right-sign $D^0 \rightarrow K^+\pi^-\pi^+\pi^-$ decays is extracted in ten bins of D^0 decay time by performing simultaneous binned likelihood fits to Δm for subsamples split depending on the D^0 charge and whether the candidate is a wrong- or right-sign decay. The ratio is calculated in each decay time bin as $R = \sqrt{(N_{D^0}^{\mathrm{WS}} \cdot N_{\overline{D}^0}^{\mathrm{WS}})/(N_{D^0}^{\mathrm{RS}} \cdot N_{\overline{D}^0}^{\mathrm{RS}})}$, to minimise the effects of the D^* production and slow π detection efficiency. The mixing parameters are extracted from a binned χ^2 fit to $R(t)$ for two fit scenarios where the mixing parameters are unconstrained and constrained to the current world average [2]. In Fig. 5, the time-dependent ratio of wrong-sign to right-sign $D^0 \rightarrow K^+\pi^-\pi^+\pi^-$ decays is illustrated along with the no-mixing hypothesis, the unconstrained and mixing-constrained fits. The no-mixing hypothesis is excluded at 8.2σ.
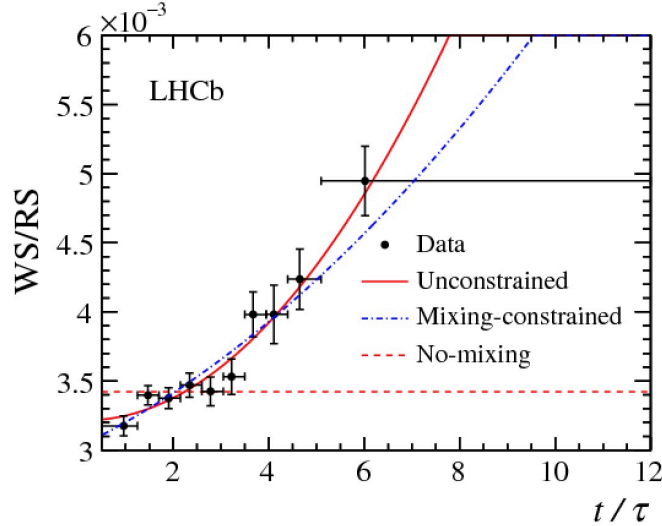

Figure 5: Time-dependent ratio of wrong-sign to right-sign $D^0 \rightarrow K^+\pi^-\pi^+\pi^-$ candidates. The no-mixing hypothesis is excluded at 8.2σ [6].

The results of the unconstrained fit are

$$r_D^{K3\pi} = (5.67 \pm 0.12) \times 10^{-2}, \tag{3.2}$$

$$R_D^{K3\pi} y'_{K3\pi} = (0.30 \pm 1.8) \times 10^{-3}, \tag{3.3}$$

$$\frac{x^2 + y^2}{4} = (4.8 \pm 1.8) \times 10^{-5}, \tag{3.4}$$

and for the mixing-constrained fit, the following results are obtained

$$r_D^{K3\pi} = (5.50 \pm 0.07) \times 10^{-2}, \tag{3.5}$$

$$R_D^{K3\pi} y'_{K3\pi} = (-3.0 \pm 0.7) \times 10^{-3}. \tag{3.6}$$

The dominant systematics arise from hadron misidentification, from charm and secondary backgrounds and from fake tracks reconstructed as slow pion from the D^* decay. The mixing-constrained fit further allows to determine lines of possible solutions in the $(\delta_D^{K3\pi}, R_D^{K3\pi})$ shown in Fig. 6.
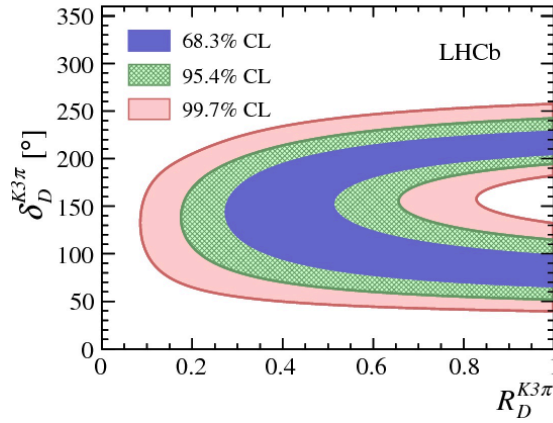

Figure 6: Constraints on the strong phase difference $\delta_D^{K3\pi}$ depending on the coherence factor $R_D^{K3\pi}$ [6].

4. Conclusion and outlook

The latest measurements published by the LHCb collaboration on charm mixing exploit novel analysis techniques and extend the existing measurements to four-body final states. The first model-independent measurement of the charm mixing parameters in $D^0 \to K_S^0 \pi^+ \pi^-$ decays found $x = (-0.86 \pm 0.53 \pm 0.17) \times 10^{-2}$ and $y = (0.03 \pm 0.46 \pm 0.13) \times 10^{-2}$. This result is a promising proof-of-principle, which will lead to a highly improved sensitivity due to now established dedicated trigger algorithms. For the first time, mixing has been established with a significance of 8.2σ in a four-body final state. In addition, the analysis of $D \to K^{\mp} \pi^{\pm} \pi^{\mp} \pi^{\pm}$ decays provides crucial input for a measurement of the CKM angle γ in $B^{\pm} \to DK^{\pm}$ with $D \to K^{\mp} \pi^{\pm} \pi^{\mp} \pi^{\pm}$ decays. With the restart of the LHC in 2015, the existing measurements will be extended to include the dataset, which is being collected until the end of 2018, to surpass the current sensitivities on charm mixing.

References

[1] PRD 2 (1970) 1285

[2] arXiv:1412.7515 [hep-ex] and online update at http://www.slac.stanford.edu/xorg/hfag

[3] JINST 3 (2008) S08005

[4] PRD 82 (2010) 112006, preprint: arXiv:1010.2817 [hep-ex]

[5] JHEP 04 (2016) 033, preprint: arXiv:1510.01664 [hep-ex]

[6] PRL 116 (2016) 241801, preprint: arXiv:1602.07224 [hep-ex]